ENVIRONMENTAL RESEARCH
LETTERS

LETTER • OPEN ACCESS

Resilience of Amazon rainfall to CO_2 removal forcing

To cite this article: Suqin Zhang *et al* 2024 *Environ. Res. Lett.* **19** 014073

ENVIRONMENTAL RESEARCH
LETTERS

LETTER

Resilience of Amazon rainfall to CO_2 removal forcing

Suqin Zhang[1,5], **Xia Qu**[1,2,4,*], **Gang Huang**[1,3,5,*], **Peng Hu**[6,7], **Xianke Yang**[8], **Ya Wang**[1] and **Liang Wu**[4,5]

[1] State Key Laboratory of Numerical Modeling for Atmospheric Sciences and Geophysical Fluid Dynamics, Institute of Atmospheric Physics, Chinese Academy of Sciences, Beijing, People's Republic of China
[2] Key Laboratory of Meteorological Disaster (KLME), Ministry of Education & Collaborative Innovation Center on Forecast and Evaluation of Meteorological Disasters (CIC-FEMD), Nanjing University of Information Science & Technology, Nanjing, People's Republic of China
[3] Laboratory for Regional Oceanography and Numerical Modeling, Qingdao National Laboratory for Marine Science and Technology, Qingdao, People's Republic of China
[4] Center for Monsoon System Research, Institute of Atmospheric Physics, Chinese Academy of Sciences, Beijing, People's Republic of China
[5] University of Chinese Academy of Sciences, Beijing, People's Republic of China
[6] Yunnan Key Laboratory of Meteorological Disasters and Climate Resources in the Greater Mekong Subregion, Yunnan University, Kunming, People's Republic of China
[7] Department of Atmospheric Sciences, Yunnan University, Kunming, People's Republic of China
[8] MOA Key Laboratory of Crop Ecophysiology and Farming System in the Middle Reaches of the Yangtze River, College of Plant Science and Technology, Huazhong Agricultural University, Wuhan, People's Republic of China
[*] Authors to whom any correspondence should be addressed.

E-mail: quxia@mail.iap.ac.cn and hg@mail.iap.ac.cn

Keywords: CO_2 removal, Amazon rainfall, moist static energy

Supplementary material for this article is available online

OPEN ACCESS

RECEIVED
7 June 2023

REVISED
22 November 2023

ACCEPTED FOR PUBLICATION
28 December 2023

PUBLISHED
11 January 2024

Abstract

Over the Amazon region, rainfall-induced changes to CO_2 pathways significantly impact humans and multiple ecosystems. Its resilience is of vital importance, and idealized CO_2 removal experiments indicate that declining trends in rainfall amounts are irreversible and exhibit a deficiency when the CO_2 concentration returns to the pre-industrial level. The irreversible decline in Amazon rainfall is mainly due to the weakened ascent, further led by two main causes. (1) Enhanced tropospheric warming and a wetter atmospheric boundary layer over the tropics during CO_2 removal generate a strong meridional gradient of temperature and specific humidity; driven by prevailing northeasterly winds, negative moist enthalpy advection occurs, which in turn weakens the ascent over the Amazon and results in anomalous drought. (2) The enhanced radiative cooling of atmospheric column. Driven by the negative lapse-rate feedback, the outgoing longwave radiative flux increases in the clear-sky atmosphere. As a result, the anomalous diabatic descent generates to maintain the energy balance of the atmospheric column. This result implies that the symmetric removal of CO_2 does not guarantee full recovery of regional precipitation.

1. Introduction

The Amazon rainforest, the world's largest tropical rainforest, stores approximately 100 Pg carbon and is home to 10%–15% of terrestrial biodiversity (Langenbrunner *et al* 2019, Jiang *et al* 2021, Boulton *et al* 2022, Wang and Huang 2022). It is an important regulator of the global climate and is recognized as a potential tipping element in the Earth system (Lenton *et al* 2009, Boulton *et al* 2013, Wang and Huang 2022). However, anthropogenic global warming is increasing tree mortality and propelling rainforest loss (Cox *et al* 2000, 2008, Gatti *et al* 2021, Bauman *et al* 2022, Boulton *et al* 2022), which is causing the resilience of the rainforest, typically defined as the return rate from perturbation to diminish (Verbesselt *et al* 2016, Zemp *et al* 2017, Yi and Jackson 2021, Boulton *et al* 2022). Since the early 2000s, resilience loss has been found in more than 75% of the Amazon rainforest (Boulton *et al* 2022, Forzieri *et al* 2022). The Amazon rainforest cover observed in 2019 was already reduced by almost 20% when compared to the coverage area that existed in 1988 (Davidson *et al* 2012, Aguiar *et al* 2016, Zemp *et al* 2017). Under a business-as-usual scenario, deforestation would reach approximately 45% of the original extent of the forest by 2050,

while longer-term deforestation would likely reach up to 100% (Zemp *et al* 2017). Climate change accelerates the loss of the Amazon rainforest by increasing the length of the dry season (Fu *et al* 2013, Adams *et al* 2017), drought frequency (Boulton *et al* 2022), and fire activity (Brando *et al* 2020, Wang and Huang 2022). Such loss leads to weaker carbon uptake and an acceleration of the atmospheric CO_2 growth rate, which forms positive feedback between the biosphere and atmosphere, and further exacerbates global warming.

Among the climate factors influencing the resilience of the Amazon rainforest, rainfall is particularly important. Several studies have suggested that the loss of resilience is faster in regions that receive less rainfall (Brando *et al* 2014, Verbesselt *et al* 2016, Bauman *et al* 2022, Boulton *et al* 2022, Forzieri *et al* 2022). During several once-in-a-century drought events (e.g. 2015), the Amazon experienced a higher rate of tree mortality under drought stress, exhibiting a more severe loss of resilience (Tomasella *et al* 2008, Phillips *et al* 2009, Allen *et al* 2010, Lewis *et al* 2011, Saatchi *et al* 2013, Brando *et al* 2014, Bi *et al* 2016, Verbesselt *et al* 2016, McDowell *et al* 2018, Aleixo *et al* 2019). Drought not only reduces ecosystem respiration (Meir *et al* 2008, Doughty *et al* 2015, Thakur *et al* 2018) and causes tree mortality through 'hydraulic failure' (Bréda *et al* 2006) or 'carbon starvation' (McDowell *et al* 2008), but also indirectly affects tree death by increasing pest and disease disturbance (Kurz *et al* 2008, Seidl *et al* 2018), as well as the occurrence of fires (Brando *et al* 2014, Gatti *et al* 2014). Tree mortality weakens forest-rainfall feedback and promotes further drought occurrence (Staal *et al* 2020). Consequently, the resilience of the Amazon rainforest will likely diminish (Forzieri *et al* 2022) under global warming scenarios.

Given the importance of rainfall to the Amazon rainforest, it is essential to understand changes in rainfall over the Amazon, especially the changes during the vegetation growing season (December–February) (Xie *et al* 2022). Previous studies on the Amazon rainfall mainly focused on the current climate and global warming scenario (Pascale *et al* 2019, Thome Sena and Magnusdottir 2020, Almazroui *et al* 2021, Liu *et al* 2022, Torres *et al* 2022), and various driving factors have been identified. For example, El Niño is typically accompanied by drought in the Amazon, which is modulated by the Walker circulation or extratropical Rossby wave train related atmospheric circulation anomalies (Cai *et al* 2020). Moreover, the impact of ENSO on Amazon rainfall is projected to intensify under global warming. Additionally, the altered Madden-Julian Oscillation could also impact Amazon rainfall through teleconnection (Liu *et al* 2022). However, the 2015 Paris Agreement proposed a target of, 'holding the increase in the global average temperature to well below 2 °C above pre-industrial (PI) levels and pursuing efforts to limit the temperature increase to 1.5 °C above PI'. Toward this target, it is necessary to remove CO_2 from the atmosphere (Peters *et al* 2013, Field and Mach 2017, Rogelj *et al* 2018, Wang *et al* 2021, Huang *et al* 2022). If CO_2 removal (CDR) methods are applied, the atmospheric CO_2 concentration will peak in this century and then continue to decline. Therefore, there has been great interest in the climate effects of CDR. Several studies have focused on understanding the hysteresis and reversibility of climate systems under a CDR scenario (Wu *et al* 2014, Kim *et al* 2022, Kug *et al* 2022, Park and Kug 2022, Schwinger *et al* 2022, Song *et al* 2022, Zhang *et al* 2023). One of the most important climate changes under the CDR scenario is that the surface temperature and precipitation in most areas of the world experience irreversible and hysteretic responses (Kim *et al* 2022) due to heat accumulated in the deep oceans during the previous stage. This indicates that changes in the global hydrological cycle under current global warming cannot be reversed even if the CO_2 concentration is reduced. Considering this, we speculate that the Amazon, with drying trends under global warming (Almazroui *et al* 2021), may have been drier during the CDR period. The rainfall in the Amazon region can remarkably influence the Amazon rainforest, so studies on how Amazon rainfall would respond under the CDR scenario are strongly desired. How does the resilience of Amazon rainfall behave in the vegetation growth season? That is, whether Amazon rainfall is able to recover to the initial condition when CO_2 returns to its PI concentration. Furthermore, possible causes of the changes in Amazon rainfall need to be resolved in more detail.

2. Data and methods

2.1. Data

In this study, the observational and reanalysis products employed are (1) Global Precipitation Climatology Project (GPCP) precipitation data (Adler *et al* 2003), and (2) National Centers for Environmental Prediction-Department of Energy (NCEP-DOE) reanalysis data, including wind variables (Kanamitsu *et al* 2002). The monthly mean variables are adopted. All the above datasets cover a common period of 1979–2014, with a horizontal resolution of 2.5° × 2.5°.

As listed in table S1, four experiments from the Coupled Model Intercomparison Project six (CMIP6) are used, including historical experiment, piControl experiment, 1%CO_2 experiment, and 1%CO_2-CDR experiment (Eyring *et al* 2016, Keller *et al* 2018). Both the 1%CO_2 and 1%CO_2-CDR experiments are 140 years in length, and are referred to as the CO_2 ramp-up and ramp-down experiments. The 1st year in the 1%CO_2 experiment is defined as Year 1. Eight available models, including ACCESS-ESM1-5, CanESM5, CESM2, CNRM-ESM2-1, GFDL-ESM4,

MIROC-ES2L, NorESM1-LM, and UKESM1-0-LL, were used in this work. Vertical velocity data, surface upwelling radiation data, and top of atmosphere (TOA) incident shortwave radiation data in UKESM1-0-LL are not available. The surface upwelling radiation data of CESM2 is not available.

To obtain the Multi-Model Ensemble (MME), we interpolated the outputs onto a $1^\circ \times 1^\circ$ grid. The ensemble spread range among the eight models was defined as $1.96 \times$ standard deviation. The results were deemed robust if more than 75% of the members (6 out of 8) display the same sign as the MME. The anomalies are the outputs of the CO_2 ramp-up and ramp-down experiments subtracted by the climatology of the last 100 years in the piControl experiment. The statistical significance of the mean difference was assessed by the two-sided Student's t test. The 21 year running mean was employed to remove interannual variability. The boreal winter (December–February) average was analyzed when the vegetation growth over the Amazon was mainly concentrated.

2.2. The resilience of Amazon rainfall

The resilience of Amazon rainfall is defined as whether the Amazon rainfall can recover to the pre-industrial level by removing the atmospheric CO_2 concentration. During the CO_2 removal period, the extent to which Amazon rainfall recovers to pre-industrial level, $AR(t)$, is expressed as the ratio of the change in rainfall relative to the CO_2 peaks to the change in rainfall during the CO_2 ramp-up period. Therefore, the equation is written as follows:

$$AR(t) = \frac{R_t - R_{140}}{R_{140} - R_{\mathrm{PI}}} \times 100, t > 140 \qquad (1)$$

R_{140}, R_{PI} represent the Amazon rainfall at the CO_2 peaks and pre-industrial levels. R_t is the Amazon rainfall at a given year t during the CO_2 removal period. A stable $AR(t) \leqslant 0$ indicates that the Amazon rainfall is recovering to the pre-industrial level. Figure 1 illustrates the related variables in formula (1).

2.3. The moisture budget

To explore the reasons for the rainfall responses over the Amazon, a simplified moisture budget equation was employed (Huang *et al* 2013):

$$\Delta P \sim -(\Delta q_{850} \cdot \omega_{500} + \Delta\omega_{500} \cdot q_{850}) \qquad (2)$$

where Δ indicates the anomalies relative to the PI level. P, q_s, and ω_{500} are precipitation, specific humidity at 850 hPa, and pressure velocity at 500 hPa, respectively. The terms on the right-hand side of the equation (2) represent the thermodynamic term related to the moisture changes ($-\Delta q_{850} \cdot \omega_{500}$) and the dynamic term related to the circulation changes ($-\Delta\omega_{500} \cdot q_{850}$). The nonlinear processes and horizontal advection term of water vapor were omitted here because they are tiny in the tropics (Held and Soden 2006, Seager *et al* 2010).

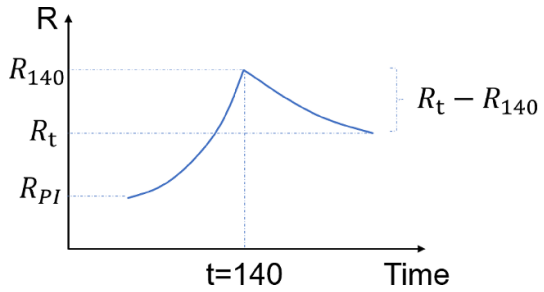

Figure 1. Illustration of the definition of Amazon rainfall resilience (formula (1)). R_{140}, R_{PI} represent the Amazon rainfall at the CO_2 peaks and pre-industrial levels, respectively. R_t is the Amazon rainfall at a given year t during the CO_2 removal period. A stable $AR(t) \leqslant 0$ indicates that the Amazon rainfall is recovering to the pre-industrial level.

2.4. The moist static energy (MSE) budget

Vertical velocity is constrained by the MSE balance in the tropics (Neelin and Held 1987). Because the seasonal mean time tendency of anomalous MSE can be neglected, the simplified anomalous MSE equation was employed:

$$\langle \omega' \cdot \partial_p \bar{h} \rangle = -\langle \bar{\omega} \cdot \partial_h h' \rangle - \langle \bar{\vec{V}} \cdot \nabla_h k' \rangle - \langle \vec{V}' \cdot \nabla_h \bar{k} \rangle + F'_{\mathrm{net}} + NL \qquad (3)$$

where MSE is $h = C_p T + L_v q + \Phi$ and moist enthalpy is represented by $k = C_p T + L_v q$. The superscript $'$, overbar $-$, and angle bracket $\langle\rangle$ represent the anomaly, the mean, and the mass-weighted vertical integration from surface to 100 hPa, respectively. ω, C_p, T, q, L_v, Φ, and NL are the pressure velocity, specific heat at constant pressure, air temperature, specific humidity, latent heat of vaporization, geopotential height, and nonlinear term, respectively. Moreover, F_{net} is the net energy flux into the atmospheric column from the surface and TOA, which is equal to

$$F'_{\mathrm{net}} = S_t^{\downarrow\prime} - S_t^{\uparrow\prime} - S_s^{\downarrow\prime} + S_s^{\uparrow\prime} - R_t^{\uparrow\prime} - R_s^{\downarrow\prime} + R_s^{\uparrow\prime} + SH' + LH' \qquad (4)$$

where S, R are the shortwave and longwave radiative flux. SH and LH are the sensible and latent flux. The subscripts s and t denote the surface and TOA, respectively. The superscript arrows ($\uparrow$ and $\downarrow$) represent the direction of radiative fluxes. For all these terms in equation (4), the positive value implied that the atmospheric column gained heat. Namely, the downward direction at the TOA and the upward direction at the surface were positive. The sum of the first seven terms on the right-hand side of equation (4) is the radiative flux, of which the first four terms can be combined as the net shortwave radiation flux (S'_{net}), and the last three can be combined as the net longwave radiation (R'_{net}). The net longwave radiation can be further divided into clear-sky (R'_{clear}) and

cloud-related (R'_{cloud}) terms. Therefore, equation (4) can be simplified to

$$F'_{net} = S'_{net} + R'_{clear} + R'_{cloud} + SH' + LH'. \quad (5)$$

In the Amazon, where active deep convection prevails, the vertical profile of anomalous vertical velocity (ω') shows a top-heavy structure with a maximum at approximately 400 hPa (figure S1), which is classified as the deep mode of tropical vertical motion (Back and Bretherton 2009). In contrast, the vertical profile of climatological MSE (h) exhibits a bottom-heavy structure, and its maximum value is at approximately 800 hPa (figure S1). According to previous studies, in the tropics, the ascending motion of the deep mode typically exports the MSE out of the atmospheric column, causing an increase in gross moisture stability (Back and Bretherton 2009). If the summation of the terms on the right-hand side of equation (3) is negative (positive), corresponding to the reduced (increased) MSE in the column, the anomalous descending (ascending) would be generated to decrease (increase) the MSE exported out of the column and thus maintain the balance of the MSE budget.

2.5. Evaluation of the CMIP6 rainfall

Before investigating the resilience of Amazon rainfall to idealized CO_2 forcing, the reproducibility of the CMIP6 models on Amazon rainfall is evaluated. Here, we compared the climatological observed rainfall with the MME of historical experiments in CMIP6.

The observed result exhibited heavy rainfall in the Amazon, with a maximum of approximately 11 mm d^{-1} (figure S2). The CMIP6 MME can grasp this spatial distribution, although the rainfall center was slightly southeastward and was stronger. The spatial correlations between individual models and observation all exceeded 0.9, with the highest correlation at 0.96 for CMIP6 MME (figure S3). Moreover, the northeast wind prevails in the Amazon in winter, which can be well reproduced by the CMIP6 MME. The above evaluation suggested that the CMIP6 MME is sufficient to investigate the resilience of Amazon rainfall to symmetric CO_2 removal.

3. Results

3.1. Irreversible change in Amazon rainfall under the CDR scenario

As shown in figure 1(a), the Amazon rainfall change is asymmetric and lags behind the evolution of the CO_2 concentration in the CO_2 ramp-up and ramp-down experiments. Amazon rainfall is defined as the regional average of land rainfall over the key domain (17.5 °S–7.5 °N, 70 °W–55 °W; red rectangles in figure 2). It decreases as the CO_2 concentration increases; after CO_2 peaks, this decline persists for approximately 25 years, up to 18% of the rainfall as that during the PI period. Thereafter, Amazon rainfall begins to recover at 40th year during the CO_2 ramp-down period (figure S4). However, this recovery is gradual and only about 71.1% (25–75 percentile: 62.86%–83.35%) of increased rainfall has been recovered when the CO_2 concentration returns to the PI level (figure S4), with anomalous drought compared to that of the PI level. To show the spatial distribution associated with the regionally averaged rainfall anomalies, two periods of the same CO_2 concentration were selected to analyze the resilience of Amazon rainfall: years 1–40 in the CO_2 ramp-up period (hereafter RU) and years 240–279 in the CO_2 ramp-down period (hereafter RD; gray bands in figure 2(a)). Precipitation change is insignificant in the Amazon during the RU period (figure 2(b)); however, during the RD period, it shows a significant deficiency compared to PI levels (figure 2(c)). Even with the same CO_2 concentration, the Amazon is significantly drier during the RD period (figure 2(d)). Overall, the simulation results imply that if the symmetrical CDR is implemented, Amazon rainfall is irreversible and may exhibit drier conditions when the CO_2 concentration returns to the unperturbed PI level.

To explore the cause of the irreversible response of Amazon rainfall, a simplified moisture budget equation, which divides the precipitation into thermodynamic ($-\Delta q_{850} \cdot \omega_{500}$) and dynamic ($-\Delta\omega_{500} \cdot q_{850}$) terms, is applied (equation (2)). The differences in these two terms between the RD and RU periods are shown in figure 3. The summation of the thermodynamic and dynamic terms reproduces the equivalent changes in rainfall (figure 3(c); figure 2(d)), further indicating a good approximation of equation (2) for the tropics (Zhou *et al* 2022). The thermodynamic component (figure 3(a)) represents the 'wet-get-wetter' mechanism, with the increased precipitation over the climatological rain band where upward motion prevails. In contrast, the dynamic component (figure 3(b)) is generally opposite to the thermodynamic component, and the amplitude is much larger. Moreover, the spatial pattern of the dynamic term bears a close resemblance to the change in precipitation (figure 2(d)). As a result, the anomalous drought conditions in the Amazon during the RD period relative to the RU period are mainly led by the dynamic component. The weakening of the ascent in the Amazon during the RD period relative to the RU period leads to the irreversible response of Amazon rainfall, as well as anomalous drier conditions locally.

3.2. Physical mechanisms behind the irreversible response

Moisture budget analysis suggests that the drier condition in the Amazon is caused by the weakened ascent during the RD period. Below, the cause of the weakened vertical velocity is explored further from

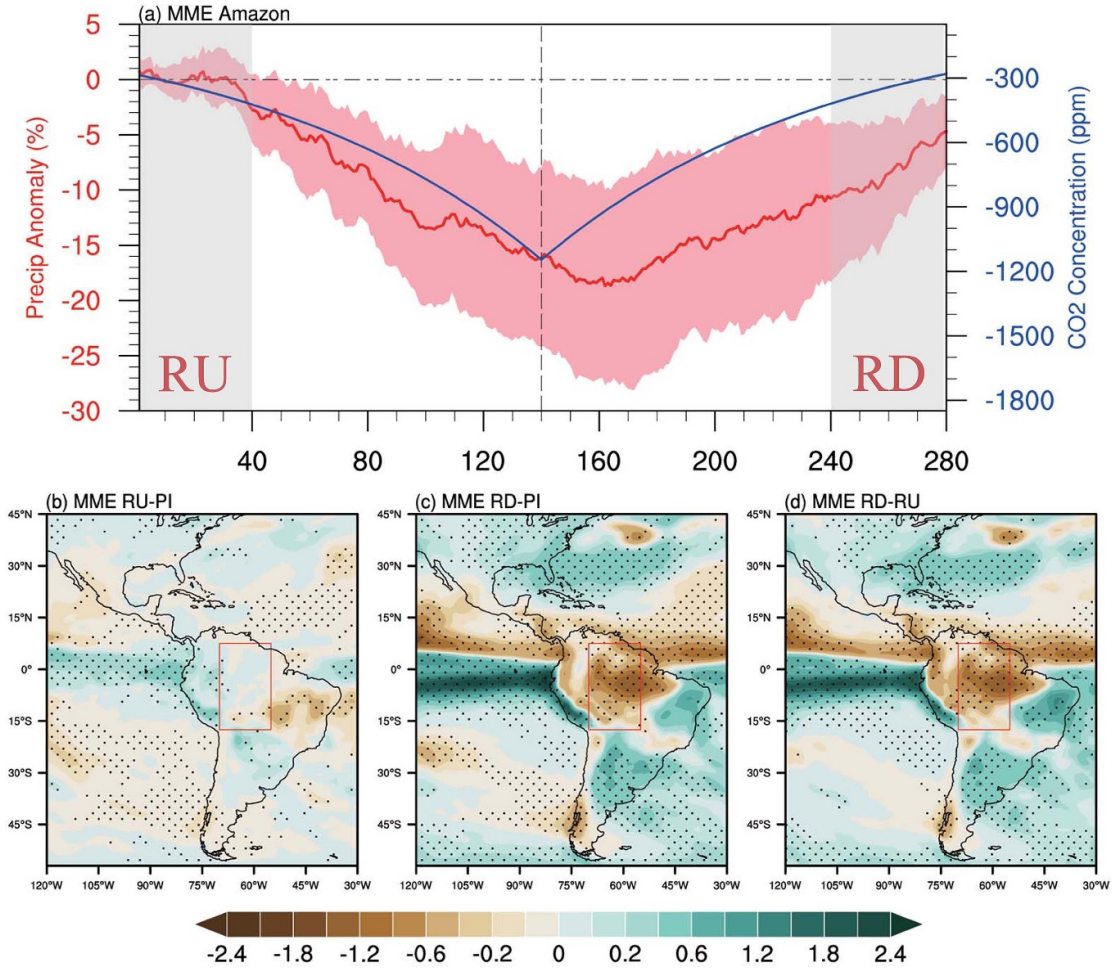

Figure 2. Evolution (a) and spatial pattern (b)–(d) of the Amazon rainfall response in CO_2 ramp-up and ramp-down experiments. (a) Time series of the CO_2 concentration (blue line; multiplied by −1 for better display; unit: ppm) and anomalous rainfall (red line; unit: mm d^{-1}). The vertical dashed line denotes the CO_2 peak year. Pink shadings indicates the 1.96 × standard deviation for the eight model members. The interannual variability is removed by 21 year running means. Two vertical gray bands in Years 1–40 (RU) and Years 240–279 (RD) are the two 40 year periods with the same average CO_2 concentration. (b) and (c) are the anomalous precipitation patterns during the RU and RD periods, respectively. (d) Is the difference between (c) and (b). Black dots in (b), (c) denote that the sign agreement test is satisfied. Black dots in (d) indicate the regions where the 75% sign agreement test is satisfied and the average difference between the RU and RD periods is statistically significant at a 90% confidence level. The Amazon region is marked by red boxes.

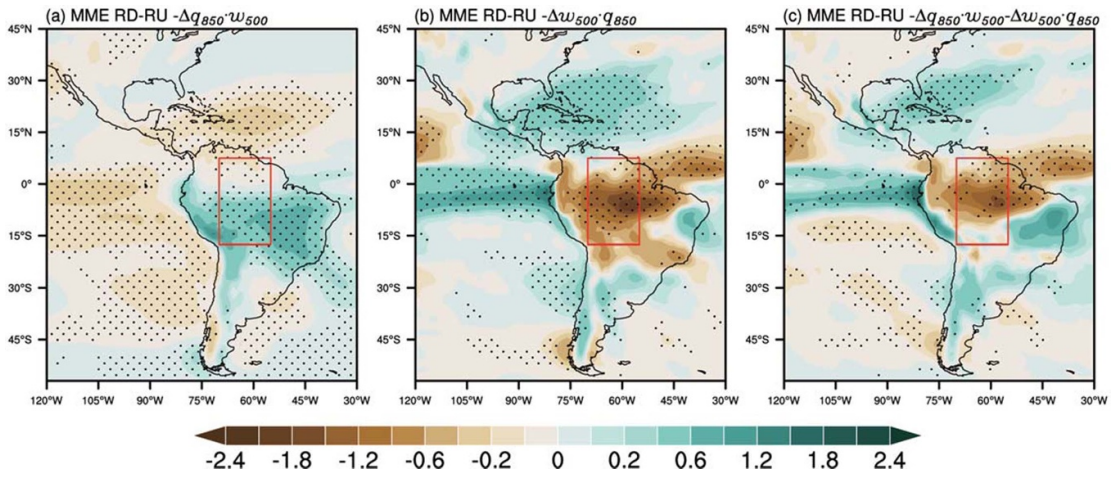

Figure 3. The difference in the thermodynamic component (a), dynamic component (b), and their sum (c) between the RU and RD periods. The units are: mm d^{-1}. The dots indicate the grids at which more than 75% of the models have the same sign as those of MME. The red boxes are the same as in figure 2(a).

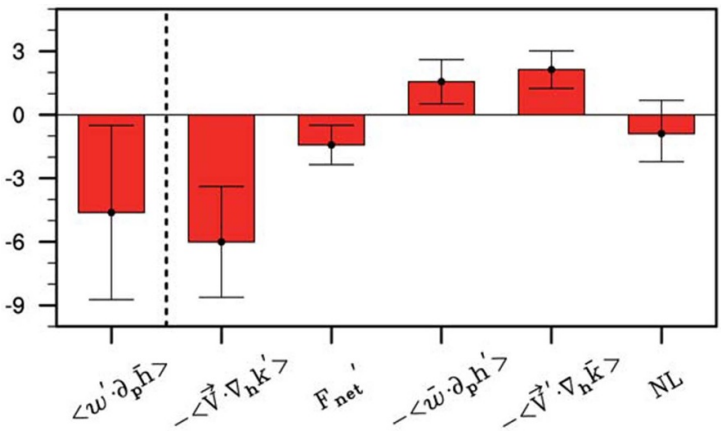

Figure 4. The difference in the terms in the MSE budget equation (unit: W m^{-2}) over the Amazon (red rectangles in figure 2) between RD and RU periods. The error bars reflect the ensemble spread of the eight models.

the view of MSE balance. The anomalous descending motion in the deep convection region over the Amazon tends to reduce the MSE output to the atmospheric column. Namely, the vertical advection term of the climatological MSE driven by anomalous vertical motion $\langle -\omega' \cdot \partial_h \bar{h} \rangle$ is positive (figure 3; this term is multiplied by -1 in equation (3)). The results of the MSE budget analysis over the Amazon indicate that this term is primarily balanced by negative horizontal advection of anomalous moist enthalpy (MEA) driven by climatological wind ($-\langle \bar{\vec{V}} \cdot \nabla_h k' \rangle$), and net energy flux anomalies F'_{net} (figure 4 and table S1). The related physical processes are analyzed as follows.

Among the terms of the MSE budget, the MEA term contributes the most to the weakened ascending motion in the Amazon. The moisture enthalpy (k) is a function of temperature and specific humidity, so both anomalous temperature advection (figure 5(a)) and moisture advection (figure 5(b)) may lead to a weakened vertical velocity. Although the CO_2 concentrations during the RD and RU periods are the same, the global surface temperature during the latter period is warmer than that in the former period due to the ocean's large thermal inertia (Wu *et al* 2014, Sun *et al* 2021, Yeh *et al* 2021). Following an approximately moist adiabat lapse rate, the troposphere over the whole tropics shows larger warming during the RD period relative to the RU period (figure 5(c)). Meanwhile, the equatorial central-eastern Pacific exhibits enhanced El Niño-like warming (Kug *et al* 2022, Oh *et al* 2022, Song *et al* 2022, Zhou *et al* 2022), which further heats the free troposphere by equatorial wave adjustments (Su and Neelin 2002, Neelin and Su 2005). According to the Clausius–Clapeyron expression, as the troposphere warms, the atmospheric boundary layer must become moister (Held and Soden 2006, Hu *et al* 2021). Thus, in the tropics, there is a strong meridional gradient of tropospheric temperature and specific humidity at 850 hPa (Shading in figures 5(c) and (d)). Driven by the climatological northeasterly wind (figures 5(c) and (d)), cold and dry air is advected into the Amazon. Consequently, it leads to a negative MEA and a weakened ascent in the Amazon, contributing to the irreversible precipitation response under the CO_2 removal scenario.

The term F'_{net} plays a secondary role (figure 4). The Amazon is dominated by negative F'_{net}, which is mainly led by the anomalous clear-sky longwave radiation R'_{clear} and latent heat (table S1). Figure 6 shows the spatial pattern of F'_{net}, R'_{clear}, and LH'. The term R'_{clear} weakens during the RD period, which suggests an intensification of radiative cooling in the cloud-free atmosphere. To maintain the energy balance of the atmospheric column, an anomalous diabatic descent occurs (Rodwell and Hoskins 1996), which leads to drier conditions over the Amazon region. The strengthened radiative cooling of the atmospheric column can be attributed to the negative lapse-rate feedback (Colman 2003, Soden and Held 2006). The global surface warming is enhanced during the RD period compared to the RU period. Following an approximately moist adiabat lapse rate, the warming is greater in the upper troposphere than in the lower one over the Amazon, resulting in a more stable atmosphere. The enhanced warming in the upper troposphere contributes to the emission of outgoing longwave radiation, thus cooling the atmospheric column. Although this effect can be offset by the positive water vapor feedback (Held and Soden 2000, Beer and Eisenman 2022), i.e. the enhanced global surface warming allows the atmosphere to hold more water vapor, which heats the atmosphere by blocking more outgoing longwave. Eventually, the net feedback is negative, leading to the atmospheric column cooled by clear-sky longwave radiation, and thus the anomalous descent. In addition, the anomalous latent heat flux also contributes, while it is partially offset by the positive anomalies

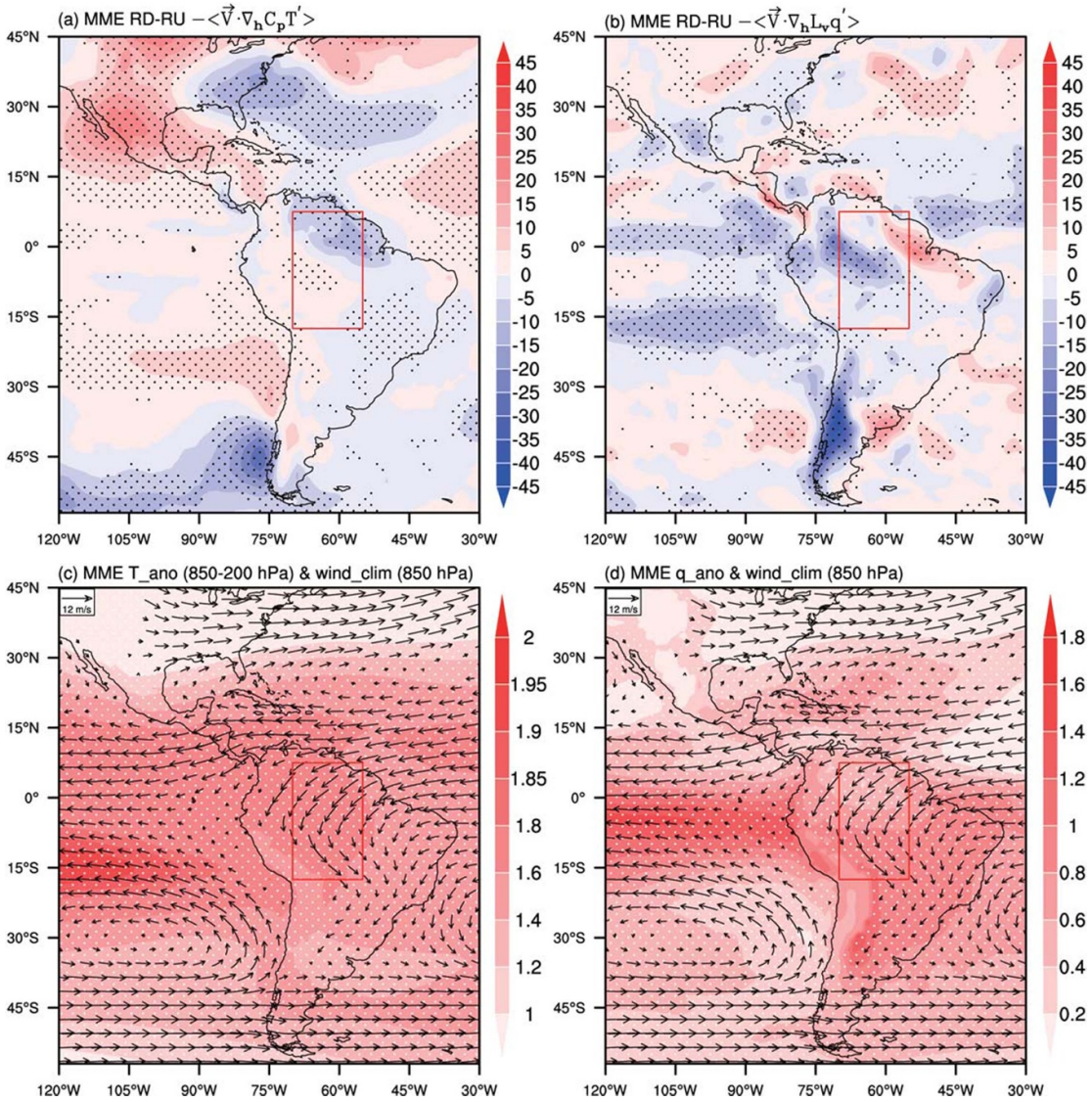

Figure 5. (a) The difference in the horizontal advection of anomalous temperature by climatological wind between the RD and RU periods (unit: W m^{-2}). (b), (c), and (d) are same as (a) but for the horizontal advection of anomalous moisture driven by climatological wind (b; unit: W m^{-2}), tropospheric-averaged (850–200 hPa) temperature anomalies (c; shading; unit: K) and 850 hPa climatological wind (c; vectors; unit: m s^{-1}), anomalous specific humidity (d; shading; unit: g kg^{-1}) and wind at 850 hPa (d; vectors; unit: m s^{-1}). The black dots and red boxes are the same as in figure 1(a). Vectors only exceeding 75% of sign consistency are shown.

of sensible heat flux (figure 6(c) and table S1). This can be explained by the terrestrial ecosystem processes associated with changes in CO_2 concentration and the climate system (Park and Kug 2022). The leaf area index (LAI), an indicator of vegetation growth, shows an opposite response in the CO_2 ramp-up and ramp-down experiments (figure S5(a)). Net primary production (NPP), i.e. net carbon uptake by vegetation, also exhibits a similar response (figure S5(b)). Compared with the RU period, the LAI and NPP are reduced in the RD period (figures S5(c) and (d)), which indicates diminished vegetation cover. As a result, evapotranspiration weakens while ventilation intensifies in the Amazon, corresponding to the weakened latent heat flux and intensified sensible heat flux during the RD period (Piao *et al* 2019, Xu *et al* 2022). Overall, the negative lapse-rate feedback and the terrestrial ecosystem feedback processes jointly amplify the irreversibility of Amazon rainfall, with anomalous drought in the RD period.

4. Summary and discussion

The resilience of Amazon rainfall in an idealized CDR simulation is investigated in this paper. It showed that if symmetric CDR is applied, Amazon rainfall decline is largely irreversible when CO_2 concentration returns to its pre-industrial level, with the Amazon incurring anomalous drought conditions. If the rainfall change is divided into thermodynamic and dynamic components, they exhibit opposite-sign contributions to the irreversible precipitation change in the Amazon. It is the weakened dynamic component associated with

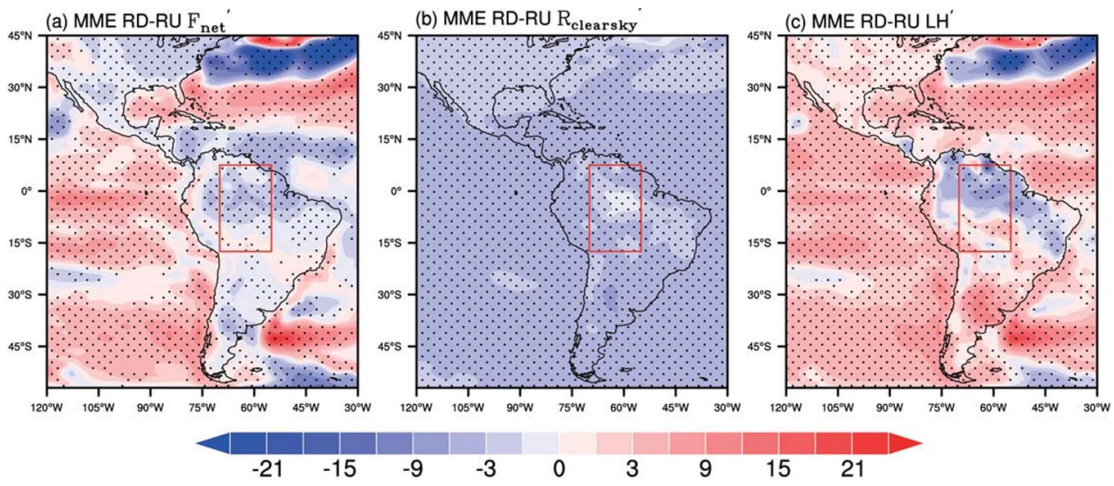

Figure 6. (a) The difference in energy flux into the atmospheric column between RD and RU periods (unit: W m^{-2}). (b), and (c) are the same as (a) but for the clear-sky longwave radiative flux, and latent heat flux, respectively (unit: W m^{-2}). The black dots and red boxes are the same as in figure 1(a).

the vertical velocity that dominates the irreversible Amazon rainfall change.

Moreover, what are the driving mechanisms behind the weakening of upward motion in the Amazon during the RD period? We attempt to resolve this issue through MSE budget analysis. The MSE budget reveals that there are two reasons for the weakened ascent in the Amazon: (1) the negative MEA $(-\langle \bar{\vec{V}} \cdot \nabla_h k' \rangle)$. The climatological northeasterly advects dry and cold air (negative MEA anomalies) to the Amazon, which reduces the MSE in the atmospheric column. Hence, the upward motion in the Amazon weakens, making it drier. (2) The negative anomalous clear-sky longwave radiative flux R'_{clear}. In the Amazon, the radiative cooling in the cloud-free atmosphere strengthens during the RD period due to the negative lapse-rate feedback. Correspondingly, an anomalous diabatic descent occurs. These two processes jointly leads to the weakened ascendance and the irreversible response of the Amazon rainfall.

In this study, we analyze the direct causes of the asymmetric response of Amazon rainfall, i.e. the negative MEA and negative radiative flux of the atmospheric column result in anomalous descent during the RD period. Essentially, the negative MEA is linked to the SST anomalies over the tropical Pacific Ocean, i.e. the enhanced El Niño-like warming. As outlined in section 3.2, our analysis reveals that this anomalous SST warming causes tropical tropospheric warming and contributes to the negative MSE. For the formation of enhanced El Niño-like warming during the CO_2 ramp-down period, previous studies attributed it largely to the lagged recovery of subthermocline ocean temperature and the Walker circulation (Song *et al* 2022, Zhou *et al* 2022, Zhang *et al* 2023). During the CO_2 removal period, the subthermocline ocean warms stronger than the upper one, which generally weakens the vertical temperature gradient and reduces the cooling effect led by the climatological upwelling in the central and eastern Pacific. Moreover, the Walker circulation weakens due to temperature and precipitation constraints, accompanied by a decrease in upwelling intensity. In combination with the processes of the Walker circulation and ocean thermal stratification, the enhanced El Niño-like warming becomes more apparent during the RD period. However, the quantitative relative importance of these two processes in the formation of enhanced SST patterns remains unclear, which calls for further analysis in future work.

Our study provides implications for the impacts of CDR on Amazon rainfall. The symmetric CDR does not result in a fully recovery of Amazon rainfall, which may threaten the growth of rainforests. This indicates that the persistent impacts of CO_2 should be considered when developing climate mitigation pathways. In addition, the environmental conditions in the Amazon rainforest are intricate and are regulated by various climate factors, such as heat, wildfire, and El Niño-Southern Oscillation, among others (Brando *et al* 2014, Aleixo *et al* 2019). In particular, there is a strong interaction between climate and intrinsic physiological processes (Leite-Filho *et al* 2021, He *et al* 2022). Hence, more comprehensive components need to be considered when understanding the impacts of CDR on the Amazon rainforest in further studies.

Data availability statements

The monthly mean winds data are obtained from NCEP-DOE, which is available at https://psl.noaa.gov/data/gridded/data.ncep.reanalysis2.pressure.html.

The observational precipitation data is from GPCP, which is available at https://psl.noaa.gov/data/gridded/data.gpcp.html.

The CMIP6 outputs are available online at https://esgf-node.llnl.gov/projects/cmip6/.

Acknowledgments

The work was supported by the National Natural Science Foundation of China (42141019, 42175055, 42261144687), the Second Tibetan Plateau Scientific Expedition and Research program (2019QZKK0102), and the project of the Key Laboratory of Meteorological Disaster, Ministry of Education & Collaborative Innovation Center on Forecast and Evaluation of Meteorological Disasters, Nanjing University of Information Science & Technology (KLME202111). The authors thank the World Climate Research Program for coordinating and promoting CMIP6, appreciate the climate modeling groups for producing and making available their model output, and are grateful to the Earth System Grid Federation (ESGF) for archiving the data and providing access.

ORCID iDs

Gang Huang https://orcid.org/0000-0002-8692-7856
Ya Wang https://orcid.org/0000-0003-1527-5413
Liang Wu https://orcid.org/0000-0001-9410-0050

References

Adams H D *et al* 2017 A multi-species synthesis of physiological mechanisms in drought-induced tree mortality *Nat. Ecol. Evol.* **1** 1285–91

Adler R F *et al* 2003 The version-2 global precipitation climatology project (GPCP) monthly precipitation analysis (1979-present) *J. Hydrometeorol.* **4** 1147–67

Aguiar A P, Vieira I C, Assis T O, Dalla-Nora E L, Toledo P M, Santos-Junior R A and Ometto J P 2016 Land use change emission scenarios: anticipating a forest transition process in the Brazilian Amazon *Glob. Change Biol.* **22** 1821–40

Aleixo I, Norris D, Hemerik L, Barbosa A, Prata E, Costa F and Poorter L 2019 Amazonian rainforest tree mortality driven by climate and functional traits *Nat. Clim. Change* **9** 384–8

Allen C D, Macalady A K, Chenchouni H, Bachelet D, McDowell N, Vennetier M and Cobb N 2010 A global overview of drought and heat-induced tree mortality reveals emerging climate change risks for forests *For. Ecol. Manage.* **259** 660–84

Almazroui M, Ashfaq M, Islam M N, Rashid I U, Kamil S, Abid M A and Sylla M B 2021 Assessment of CMIP6 performance and projected temperature and precipitation changes over South America *Earth Syst. Environ.* **5** 155–83

Back L E and Bretherton C S 2009 A simple model of climatological rainfall and vertical motion patterns over the tropical oceans *J. Clim.* **22** 6477–97

Bauman D, Fortunel C, Delhaye G, Malhi Y, Cernusak L A, Bentley L P and McMahon S M 2022 Tropical tree mortality has increased with rising atmospheric water stress *Nature* **608** 528–33

Beer E and Eisenman I 2022 Revisiting the role of the water vapor and lapse rate feedbacks in the Arctic amplification of climate change *J. Clim.* **35** 2975–88

Bi J, Myneni R, Lyapustin A, Wang Y J, Park T, Chi C and Knyazikhin Y 2016 Amazon forests' response to droughts: a perspective from the MAIAC product *Remote Sens.* **8** 356

Boulton C A, Good P and Lenton T M 2013 Early warning signals of simulated Amazon rainforest dieback *Theor. Ecol.* **6** 373–84

Boulton C A, Lenton T M and Boers N 2022 Pronounced loss of Amazon rainforest resilience since the early 2000s *Nat. Clim. Change* **12** 271–8

Brando P M, Balch J K, Nepstad D C, Morton D C, Putz F E, Coe M T and Soares-Filho B S 2014 Abrupt increases in Amazonian tree mortality due to drought-fire interactions *Proc. Natl Acad. Sci. USA* **111** 6347–52

Brando P M, Soares-Filho B, Rodrigues L, Assuncao A, Morton D, Tuchschneider D and Coe M T 2020 The gathering firestorm in southern Amazonia *Sci. Adv.* **6** eaay1632

Bréda N, Huc R, Granier A and Dreyer E 2006 Temperate forest trees and stands under severe drought: a review of ecophysiological responses, adaptation processes and long-term consequences *Ann. For. Sci.* **63** 625–44

Cai W J *et al* 2020 Climate impacts of the El Niño-Southern Oscillation on South America *Nat. Rev. Earth Environ.* **1** 215–31

Colman R 2003 A comparison of climate feedbacks in general circulation models *Clim. Dyn.* **20** 865–73

Cox P M, Betts R A, Jones C D, Spall S A and Totterdell I J 2000 Acceleration of global warming due to carbon-cycle feedbacks in a coupled climate model *Nature* **408** 184–7

Cox P M, Harris P P, Huntingford C, Betts R A, Collins M, Jones C D and Nobre C A 2008 Increasing risk of Amazonian drought due to decreasing aerosol pollution *Nature* **453** 212–5

Davidson E A, de Araujo A C, Artaxo P, Balch J K, Brown I F, MM C B and Wofsy S C 2012 The Amazon basin in transition *Nature* **481** 321–8

Doughty C E, Metcalfe D B, Girardin C A, Amezquita F F, Cabrera D G, Huasco W H and Malhi Y 2015 Drought impact on forest carbon dynamics and fluxes in Amazonia *Nature* **519** 78–82

Eyring V, Bony S, Meehl G A, Senior C A, Stevens B, Stouffer R J and Taylor K E 2016 Overview of the Coupled Model Intercomparison Project Phase 6 (CMIP6) experimental design and organization *Geosci. Model Dev.* **9** 1937–58

Field C B and Mach K J 2017 Rightsizing carbon dioxide removal *Science* **356** 706–7

Forzieri G, Dakos V, McDowell N G, Ramdane A and Cescatti A 2022 Emerging signals of declining forest resilience under climate change *Nature* **608** 534–9

Fu R, Yin L, Li W, Arias P A, Dickinson R E, Huang L and Myneni R B 2013 Increased dry-season length over southern Amazonia in recent decades and its implication for future climate projection *Proc. Natl Acad. Sci. USA* **110** 18110–5

Gatti L V, Basso L S, Miller J B, Gloor M, Gatti Domingues L, Cassol H L G and Neves R A L 2021 Amazonia as a carbon source linked to deforestation and climate change *Nature* **595** 388–93

Gatti L V, Gloor M, Miller J B, Doughty C E, Malhi Y, Domingues L G and Lloyd J 2014 Drought sensitivity of Amazonian carbon balance revealed by atmospheric measurements *Nature* **506** 76–80

He M Z, Piao S L, Huntingford C, Xu H, Wang X H, Bastos A and Gasser T 2022 Amplified warming from physiological responses to carbon dioxide reduces the potential of vegetation for climate change mitigation *Commun. Earth Environ.* **3** 160

Held I M and Soden B J 2000 Water vapor feedback and global warming *Annu. Rev. Energy Environ.* **25** 441–75

Held I M and Soden B J 2006 Robust responses of the hydrological cycle to global warming *J. Clim.* **19** 5686–99

Hu K M, Huang G, Huang P, Kosaka Y and Xie S P 2021 Intensification of El Niño-induced atmospheric anomalies under greenhouse warming *Nat. Geosci.* **14** 377–82
Huang G, Xu Z, Qu X, Cao J, Long S, Yang K and Ma X 2022 Critical climate issues toward carbon neutrality targets *Fundam. Res.* **2** 396–400
Huang P, Xie S P, Hu K M, Huang G and Huang R H 2013 Patterns of the seasonal response of tropical rainfall to global warming *Nat. Geosci.* **6** 357–61
Jiang X, Li K F, Liang M C and Yung Y L 2021 Impact of Amazonian fires on atmospheric CO_2 *Geophys. Res. Lett.* **48** 2020GL091875
Kanamitsu M, Ebisuzaki W, Woollen J, Yang S K, Hnilo J J, Fiorino M and Potter G L 2002 NCEP-DOE AMIP-II reanalysis (R-2) *Bull. Am. Meteorol. Soc.* **83** 1631–43
Keller D P, Lenton A, Scott V, Vaughan N E, Bauer N, Ji D Y and Zickfeld K 2018 The Carbon Dioxide Removal Model Intercomparison Project (CDRMIP): rationale and experimental protocol for CMIP6 *Geosci. Model Dev.* **11** 1133–60
Kim S K, Shin J, An S I, Kim H J, Im N, Xie S P and Yeh S W 2022 Widespread irreversible changes in surface temperature and precipitation in response to CO_2 forcing *Nat. Clim. Change* **12** 834–40
Kug J S, Oh J H, An S I, Yeh S W, Min S K, Son S W and Shin J 2022 Hysteresis of the intertropical convergence zone to CO_2 forcing *Nat. Clim. Change* **12** 47–53
Kurz W A, Stinson G, Rampley G J, Dymond C C and Neilson E T 2008 Risk of natural disturbances makes future contribution of Canada's forests to the global carbon cycle highly uncertain *Proc. Natl Acad. Sci. USA* **105** 1551–5
Langenbrunner B, Pritchard M S, Kooperman G J and Randerson J T 2019 Why does Amazon precipitation decrease when tropical forests respond to increasing CO_2? *Earth's Future* **7** 450–68
Leite-Filho A T, Soares-Filho B S, Davis J L, Abrahao G M and Borner J 2021 Deforestation reduces rainfall and agricultural revenues in the Brazilian Amazon *Nat. Commun.* **12** 2591
Lenton T M, Held H, Kriegler E, Hall J W, Lucht W, Rahmstorf S and Schellnhuber H J 2009 Tipping elements in the Earth's climate system *Proc. Natl Acad. Sci. USA* **105** 1786–93
Lewis S L, Brando P M, Phillips O L, van der Heijden G M and Nepstad D 2011 The 2010 Amazon drought *Science* **331** 554
Liu F, Wang B, Ouyang Y, Wang H, Qiao S, Chen G and Dong W 2022 Intraseasonal variability of global land monsoon precipitation and its recent trend *npj Clim. Atmos. Sci.* **5** 30
McDowell N, Allen C D, Anderson-Teixeira K, Brando P, Brienen R, Chambers J and Xu X 2018 Drivers and mechanisms of tree mortality in moist tropical forests *New Phytol.* **219** 851–69
McDowell N, Pockman W T, Allen C D, Breshears D D, Cobb N, Kolb T and Yepez E A 2008 Mechanisms of plant survival and mortality during drought: why do some plants survive while others succumb to drought? *New Phytol.* **178** 719–39
Meir P, Metcalfe D B, Costa A C and Fisher R A 2008 The fate of assimilated carbon during drought: impacts on respiration in Amazon rainforests *Phil. Trans. R. Soc.* B **363** 1849–55
Neelin J D and Held I M 1987 Modeling tropical convergence based on the moist static energy budget *Mon. Weather Rev.* **115** 3–12
Neelin J D and Su H 2005 Moist teleconnection mechanisms for the tropical South American and Atlantic sector *J. Clim.* **18** 3928–50
Oh H, An S I, Shin J, Yeh S W, Min S K, Son S W and Kug J S 2022 Contrasting hysteresis behaviors of Northern Hemisphere land monsoon precipitation to CO_2 pathways *Earth's Future* **10** e2021EF002623
Park S-W and Kug J-S 2022 A decline in atmospheric CO_2 levels under negative emissions may enhance carbon retention in the terrestrial biosphere *Commun. Earth Environ.* **3** 289
Pascale S, Carvalho L M V, Adams D K, Castro C L and Cavalcanti I F A 2019 Current and future variations of the monsoons of the Americas in a warming climate *Curr. Clim. Change Rep.* **5** 125–44
Peters G P, Andrew R M , Boden T, Canadell J G, Ciais P, Le Quere C and Wilson C 2013 Commentary: The challenge to keep global warming below 2 degrees C *Nat. Clim. Change* **3** 4–6
Phillips O L, Aragao L E, Lewis S L, Fisher J B, Lloyd J, Lopez-Gonzalez G and Torres-Lezama A 2009 Drought sensitivity of the Amazon rainforest *Science* **323** 1344–7
Piao S, Wang X, Park T, Chen C, Lian X, He Y and Myneni R B 2019 Characteristics, drivers and feedbacks of global greening *Nat. Rev. Earth Environ.* **1** 14–27
Rodwell M J and Hoskins B J 1996 Monsoons and the dynamics of deserts *Q. J. R. Meteorol. Soc.* **122** 1385–404
Rogelj J, Popp A, Calvin K V, Luderer G, Emmerling J, Gernaat D and Tavoni M 2018 Scenarios towards limiting global mean temperature increase below 1.5 °C *Nat. Clim. Change* **8** 325–32
Saatchi S, Asefi-Najafabady S, Malhi Y, Aragao L E, Anderson L O, Myneni R B and Nemani R 2013 Persistent effects of a severe drought on Amazonian forest canopy *Proc. Natl Acad. Sci. USA* **110** 565–70
Schwinger J, Asaadi A, Steinert N J and Lee H 2022 Emit now, mitigate later? Earth system reversibility under overshoots of different magnitude and duration *Earth Syst. Dyn.* **13** 1641–65
Seager R, Naik N and Vecchi G A 2010 Thermodynamic and dynamic mechanisms for large-scale changes in the hydrological cycle in response to global warming *J. Clim.* **23** 4651–68
Seidl R, Klonner G, Rammer W, Essl F, Moreno A, Neumann M and Dullinger S 2018 Invasive alien pests threaten the carbon stored in Europe's forests *Nat. Commun.* **9** 1626
Soden B J and Held I M 2006 An assessment of climate feedbacks in coupled ocean–atmosphere models *J. Clim.* **19** 3354–60
Song S Y, Yeh S W, An S I, Kug J S, Min S K, Son S W and Shin J 2022 Asymmetrical response of summer rainfall in East Asia to CO_2 forcing *Sci. Bull.* **67** 213–22
Staal A, Fetzer I, Wang-Erlandsson L, Bosmans J H C, Dekker S C, van Nes E H and Tuinenburg O A 2020 Hysteresis of tropical forests in the 21st century *Nat. Commun.* **11** 4978
Su H and Neelin J D 2002 Teleconnection mechanisms for tropical Pacific descent anomalies during El Niño *J. Atmos. Sci.* **59** 2694–712
Sun M A, Sung H M, Kim J, Lee J H, Shim S, Boo K O and Kim Y H 2021 Reversibility of the hydrological response in East Asia from CO_2-derived climate change based on CMIP6 simulation *Atmosphere* **12** 72
Thakur M P, Reich P B, Hobbie S E, Stefanski A, Rich R, Rice K E and Eisenhauer N 2018 Reduced feeding activity of soil detritivores under warmer and drier conditions *Nat. Clim. Change* **8** 75–78
Thome Sena A C and Magnusdottir G 2020 Projected end-of-century changes in the South American monsoon in the CESM large ensemble *J. Clim.* **33** 7859–74
Tomasella J, Nobre C A, Marengo J A, Oyama M D, Sampaio de Oliveira G, de Oliveira R and Brown I F 2008 The drought of Amazonia in 2005 *J. Clim.* **21** 495–516
Torres R R, Benassi R B, Martins F B and Lapola D M 2022 Projected impacts of 1.5 and 2 °C global warming on temperature and precipitation patterns in South America *Int. J. Climatol.* **42** 1597–611
Verbesselt J, Umlauf N, Hirota M, Holmgren M, Van Nes E H, Herold M and Scheffer M 2016 Remotely sensed resilience of tropical forests *Nat. Clim. Change* **6** 1028–31
Wang F, Harindintwali J D, Yuan Z, Wang M, Wang F, Li S and Chen J M 2021 Technologies and perspectives for achieving carbon neutrality *Innovation* **2** 100180
Wang Y and Huang P 2022 Potential fire risks in South America under anthropogenic forcing hidden by the Atlantic multidecadal oscillation *Nat. Commun.* **13** 2437

Wu P, Ridley J, Pardaens A, Levine R and Lowe J 2014 The reversibility of CO_2 induced climate change *Clim. Dyn.* **45** 745–54

Xie X, He B, Guo L, Huang L, Hao X, Zhang Y and Wang S 2022 Revisiting dry season vegetation dynamics in the Amazon rainforest using different satellite vegetation datasets *Agric. For. Meteorol.* **312** 108704

Xu X Y, Zhang X Y, Riley W J, Xue Y, Nobre C A, Lovejoy T E and Jia G S 2022 Deforestation triggering irreversible transition in Amazon hydrological cycle *Environ. Res. Lett.* **17** 034037

Yeh S W, Song S Y, Allan R P, An S I and Shin J 2021 Contrasting response of hydrological cycle over land and ocean to a changing CO_2 pathway *npj Clim. Atmos. Sci.* **4** 53

Yi C and Jackson N 2021 A review of measuring ecosystem resilience to disturbance *Environ. Res. Lett.* **16** 053008

Zemp D C, Schleussner C F, Barbosa H M J and Rammig A 2017 Deforestation effects on Amazon forest resilience *Geophys. Res. Lett.* **44** 6182–90

Zhang S, Qu X, Huang G and Hu P 2023 Asymmetric response of South Asian summer monsoon rainfall in a carbon dioxide removal scenario *npj Clim. Atmos. Sci.* **6** 6–10

Zhou S, Huang P, Xie S P, Huang G and Wang L 2022 Varying contributions of fast and slow responses cause asymmetric tropical rainfall change between CO_2 ramp-up and ramp-down *Sci. Bull.* **67** 1702–11